JACS
JOURNAL OF THE AMERICAN CHEMICAL SOCIETY
Communication
Cite This: J. Am. Chem. Soc. 2018, 140, 1235−1238
pubs.acs.org/JACS

High Drug Loading and Sub-Quantitative Loading Efficiency of Polymeric Micelles Driven by Donor−Receptor Coordination Interactions

Shixian Lv,[†,‡] Yuchen Wu,[†] Kaimin Cai,[‡] Hua He,[†] Yongjuan Li,[†] Min Lan,[†] Xuesi Chen,[§] Jianjun Cheng,[‡] and Lichen Yin*[,†]

[†]Jiangsu Key Laboratory for Carbon-Based Functional Materials and Devices, Institute of Functional Nano and Soft Materials (FUNSOM), Collaborative Innovation Center of Suzhou Nano Science and Technology, Joint International Research Laboratory of Carbon-Based Functional Materials and Devices, Soochow University, Suzhou 215123, China

[‡]Department of Materials Science and Engineering, University of Illinois at Urbana−Champaign, Urbana, Illinois 61801, United States

[§]Key Laboratory of Polymer Ecomaterials, Changchun Institute of Applied Chemistry, Chinese Academy of Sciences, Changchun 130022, China

Supporting Information

ABSTRACT: Polymeric micelles are extensively used for the delivery of hydrophobic drugs, which, however, suffer from unsatisfactory drug loading, colloidal uniformity, formulation stability, and drug release. Herein, we demonstrate a convenient strategy to prepare micelles with ultrahigh drug loading via the incorporation of polymer−drug coordination interactions. An amphiphilic copolymer containing pendant phenylboronic acid as electron acceptor unit was synthesized, which afforded donor−acceptor coordination with doxorubicin to obtain micelles with ultrahigh drug loading (~50%), nearly quantitative loading efficiency (>95%), uniform size, and colloidal stability. Besides, the encapsulated drug can be effectively and selectively released in response to the high reactive oxygen species levels in cancer cells, which potentiated the anticancer efficacy and reduced systemic toxicity. Apart from doxorubicin, the current platform could be extended to other drugs with electron-donating groups (e.g., epirubicin and irinotecan), rendering a simple and robust strategy for enabling high drug loading in polymeric micelles and cancer-specific drug release.

Micellar nanoparticles (NPs) formed via the self-assembly of amphiphilic polymers represent an important delivery platform for hydrophobic chemo-drugs.[1] Micelles with core−shell nanostructure encapsulate the hydrophobic drug in the core, and the hydrophilic shell enhances the colloidal stability in physiological fluids.[2] While polymeric nanomedicine (NM) has been extensively studied, their clinical translation is still hurdled by the various formulation challenges including drug loading, release profile, size distribution, and stability.[3] Micellar NMs usually demonstrate unsatisfactory drug loading,[4] exemplified by the typical low drug loading capacity (<5%) for chemo-drugs, such as doxorubicin (DOX) and camptothecin (CPT).[5] Although few high-drug-loading micelles have been prepared from drug−drug conjugate or prodrug, it is still of great difficulty to achieve high drug loading for most polymeric micelles.[6] In addition, unsatisfactory drug release and formulation stability greatly limit the application of polymeric micelles.[7] We herein report a facile approach to prepare polymeric micelles with quantitative loading efficiency, ultra-high drug loading, and controlled drug release via the introduction of coordination interactions between the drug and polymeric carrier.

Polymer−drug interaction dominates the formulation of drug-incorporated micelles. Hydrophobic interaction between the drug and polymer is the major driving force for drug encapsulation. However, the hydrophobic interaction is non-specific, which also occurs among free drug molecules. Therefore, undesired drug aggregation happens during the self-assembly process, which decreases the drug loading efficiency and heterogeneity of the formulation (Scheme 1a). Altering the molecular structure of chemo-drugs serves as an efficient approach to achieve high drug loading via inhibition of drug aggregation, which, however, involves complicated chemical synthesis.[8] As an alternative, enhancing the drug−

Scheme 1. Schematic Illustration of the Encapsulation of Hydrophobic Drugs into Polymeric Micelles

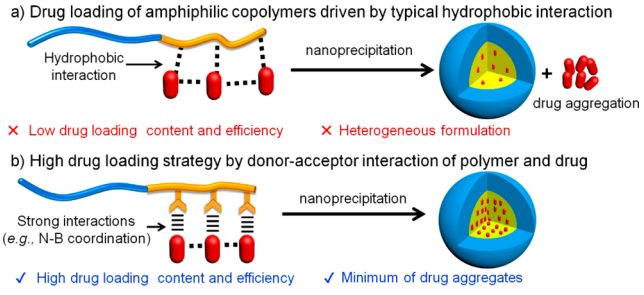

(a) Unwanted formation of drug aggregates during drug loading via hydrophobic interactions. (b) Quantitative and high drug loading enabled via specific drug−polymer coordination interactions.

Received: December 3, 2017
Published: January 13, 2018

DOI: 10.1021/jacs.7b12776
J. Am. Chem. Soc. 2018, 140, 1235−1238

polymer interaction may provide a more convenient way (Scheme 1b). To this end, introduction of suitable molecular forces that can specifically enhance the polymer−drug interaction is highly demanded.

Donor−acceptor interaction, also known as coordination bonding, is a common molecular force between electron donors and acceptors including π-donor/organometallics or Lewis bases/acids. This interaction widely exists in material systems and is extensively utilized for catalysis or assembly.[9] The donor−acceptor bond energy is usually weaker than covalent bonds whereas stronger than hydrophobic interactions. As such, we hypothesize that the donor−acceptor coordination could be incorporated into the polymer−drug interaction to yield micelles with high drug loading and uniform distribution (Scheme 1b). Because of the reversible nature of the coordination bond, it will not alter the molecular structure of drugs.[10] A wide range of Lewis acids/bases can be incorporated, which features synthetic simplicity and chemical diversity to manipulate the polymer structure for controlled drug release.

In support of such hypothesis, boronic acid, a common Lewis acid, is of particular interest due to its ability to form reversible interactions with donor atoms (e.g., oxygen and nitrogen).[9a,11] More importantly, the boronic acids/esters such as phenylboronic acid (PBA) are sensitive to reactive oxygen species (ROS) that are overproduced in cancer cells.[12] As such, PBA-incorporated amphiphilic copolymers would afford specific and strong coordination interactions with electron-donating chemodrugs to enhance their loading. In cancer cells, the excessive ROS could selectively release the drug, thus potentiating their antitumor efficacy while reducing systemic toxicity.

To realize such design strategy, we synthesized amphiphilic copolymer bearing pendant PBA moieties on the side-chain terminals of the hydrophobic segment. A noncharged and biocompatible scaffold, methoxy poly(ethylene glycol)-*b*-poly-[(*N*-2-hydroxyethyl)-aspartamide] ($mPEG_{113}$-*b*-$PHEA_{21}$) was obtained through the aminolysis of mPEG-*b*-poly(γ-benzyl-$_L$-aspartate) (mPEG-*b*-PBLA) with ethanolamine (Scheme S1, Figures S1 and S2).[13] mPEG-*b*-PHEA was modified with 4-(hydroxymethyl) phenylboronic acid pinacol carbonylimidazole to obtain amphiphilic copolymer, P-PBA (Figure 1a). The pendant PBA moieties could serve as electron acceptors for coordination interactions with chemo-drugs. As a control, mPEG-*b*-PHEA was also modified by benzyl carbonylimidazole to obtain P-CBZ that contained the hydrophobic benzyl side groups with no electron accepting capability (Figure 1a). P-PBA and P-CBZ had similar amount of hydrophobic groups on the side chains (9−10 benzyl or PBA moieties per polymer, Figures S3−S6 and Table S1), and the only difference was the electron accepting/donating capability.

DOX was selected as a model hydrophobic drug that possessed electron donor groups (primary amine) to interact with boronic acid on P-PBA. The interaction between DOX and PBA was first studied by ^{11}B NMR in deuterated dimethylformamide (DMF-d_7). PBA showed the typical chemical shift of aryl boronic acid/ester at 29−30 ppm (Figure 1b). After interaction with DOX, a peak shift to high field (~20 ppm) appeared due to coordination of PBA with the nitrogen atom of DOX.[10] The peak shift remained after addition of water, indicating aqueous stability of the coordination interaction. Subsequently, drug loading by P-CBZ and P-PBA micelles was studied using the nanoprecipitation method. Upon coprecipitation of DOX with P-CBZ at 1:1 (w/w), micrometer-sized drug precipitates immediately appeared and multiple

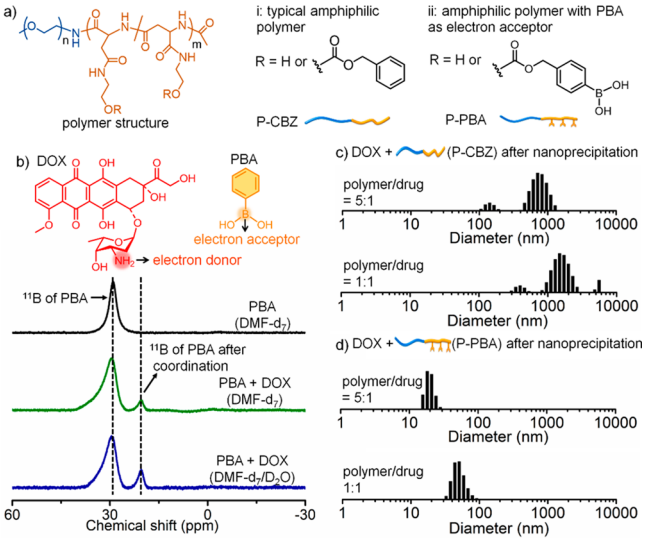

Figure 1. (a) Design of a typical amphiphilic copolymer containing electron acceptor. (b) ^{11}B NMR spectra of PBA and PBA&DOX. Intensity size distributions of DOX-loaded P-CBZ (c) and P-PBA (d) micelles.

distributions were observed in the dynamic light scattering (DLS) diagrams. Such formulation heterogeneity was still observed when the drug/polymer ratio was decreased to 1:5 (w/w) (Figure 1c). On the contrary, no large-sized precipitate was observed for P-PBA micelles, obtaining homogeneous micelles with small size (<50 nm) and monomodal distributions at various DOX/P-PBA feeding ratios (Figure 1d and Table S2). Due to excessive drug aggregation, P-CBZ micelles showed low drug loading content (DLC, ~3%) and drug loading efficiency (DLE, 7−20%). Comparatively, P-PBA micelles demonstrated dramatically improved DLC (~50%) along with ~100% DLE (Table 1). Such discrepancy clearly evidenced the advantage of coordination interaction-mediated drug loading over traditional mechanisms via hydrophobic interactions.

Table 1. DLC and DLE of Different Micelles

Micelles	Polymer	Drug/polymer (w/w)	DLC (%)	DLE (%)
PC-DOX-1	P-CBZ	1:5	3.3	19.8
PC-DOX-2	P-CBZ	1:2	3.7	11.1
PC-DOX-3	P-CBZ	1:1.5	3.5	8.8
PC-DOX-4	P-CBZ	1:1	3.3	6.6
PB-DOX-1	P-PBA	1:5	17.4	>99
PB-DOX-2	P-PBA	1:2	33.4	>99
PB-DOX-3	P-PBA	1:1.5	40.0	>99
PB-DOX-4	P-PBA	1:1	49.0	98

The distinct drug loading performance of P-CBZ and P-PBA micelles might be largely attributed to their different interactions with drug molecules. The donor−acceptor coordination between drug and P-PBA can stabilize the polymer−drug complex, eliminate drug aggregation, and thereby drive the quantitative drug loading (Scheme 1b). One possible concern was whether covalent bonds would form, which would otherwise inhibit the drug release (Scheme S2). To answer this question, we analyzed the mass spectrum of the PBA-DOX mixture in DMF, which revealed no stable covalent bonding (Figure S7). High-performance liquid chromatography

DOI: 10.1021/jacs.7b12776
J. Am. Chem. Soc. 2018, 140, 1235−1238

(HPLC) analysis further confirmed such finding. DOX/PBA mixture and PB-DOX-4 micelles showed similar elution peaks (Figures S8 and S9), probably due to destruction of the PBA-DOX coordination in the acidic mobile phase, which further demonstrated reversibility of the coordination interaction. These results collectively indicated that coordination interaction rather than covalent bonding contributed to the high drug loading, without altering the chemical structure of the drug payloads.

We next studied the lyophilization stability and serum stability of the drug-loaded micelles, two important requirements for NM. Lyophilized PB-DOX-2 micelles were well dispersed in phosphate buffered saline (PBS) at 10 mg DOX/mL (Figure S10), affording small size (<50 nm) and monomodal distribution (Table S2). Transmission electron microscopy (TEM) observation further revealed unaltered morphology and dispersity of micelles after lyophilization (Figure S11). In addition, size of the PB-DOX-2 micelles maintained constant upon 48 h of incubation in PBS with or without 10% serum (Figure S12), revealing desired colloidal stability.

Arylboronic esters could be oxidized by ROS (e.g., H_2O_2) and then undergo rearrangement to unmask the modified group (Figure 2a).[12a,14] Thus, we investigated the H_2O_2-triggered removal of PBA groups by ^{1}H NMR. Due to the core−shell structure, P-PBA micelles in D_2O only showed the PEG peak (Figure 2b). After H_2O_2 treatment, peaks of 4-(hydroxymethyl)phenol and mPEG-*b*-PHEA appeared, demonstrating disassembly of the micelles. The peak intensity of the degraded products increased with incubation time (Figure 2b), leading to removal of ∼80% PBA groups after 60-h incubation. H_2O_2 treatment (100 μM) significantly increased the size of DOX-loaded P-PBA micelles, and almost no DLS signals were detected after 48 h of incubation, indicating disassembly of the micelles (Figure S13). Consistently, H_2O_2 (100 μM) also promoted DOX release, leading to an accumulative drug release of ∼75% within 48 h (Figure 2c). As a nonresponsive analogue, DOX release from P-CBZ micelles were not affected by H_2O_2 (Figure S14). Acidic pH also accelerated the drug release from P-PBA micelles, presumably due to the protonation of DOX that destroyed the coordination interaction (Figure 2c).

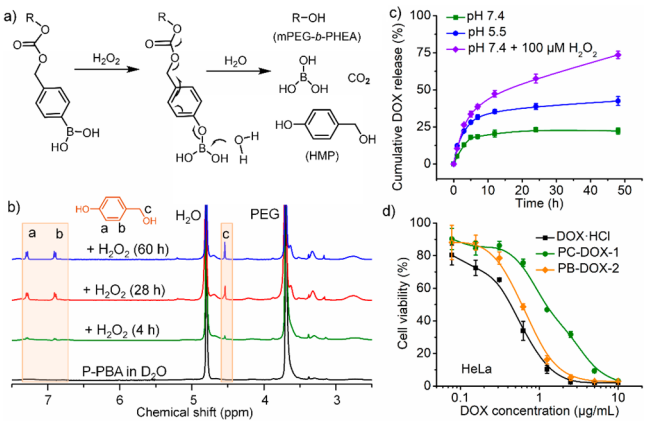

Figure 2. (a) Schematic illustration of H_2O_2-triggered removal of PBA moiety from the polymer. (b) ^{1}H NMR spectra of P-PBA micelles after H_2O_2 treatment. (c) *In vitro* drug release profiles of PB-DOX-2 micelles (n = 3). (d) Cytotoxicity of DOX-loaded micelles toward HeLa cells after 48 h of incubation (n = 3).

The *in vitro* cytotoxicity of the blank and DOX-loaded micelles was then investigated. mPEG-*b*-PHEA, P-CBZ, and P-PBA were almost nontoxic to HeLa, B16F10, HepG2, and NIH/3T3 cells at concentrations up to 1 mg/mL (Figures S15 and S16). In comparison, PB-DOX-2 micelles demonstrated dose-dependent cytotoxicity to HeLa cells (Figure 2d), achieving an IC_{50} value of 0.60 μg/mL, similar to that of free DOX (0.43 μg/mL). As a nonresponsive analogue, PC-DOX-1 micelles showed notably higher IC_{50} (1.22 μg/mL). Such discrepancy was further noted in other two cancer cell lines (HepG2 and B16F10), which was largely attributed to the ROS-mediated rapid release of DOX from PB-DOX-2 micelles but not PC-DOX-1 micelles (Figure S18). In support of such observation, PB-DOX-2 micelles only showed slightly stronger cytotoxicity than PC-DOX-1 micelles in NIH/3T3 cells (normal cell), due to the lack of intracellular ROS to trigger DOX release from PB-DOX-2 micelles (Figure S18). Because of the cancer cell-selective drug release, PB-DOX-2 micelles showed desired animal tolerance at the maximal tolerated dose (MTD) of ∼40 mg DOX/kg (Figure S19), 8-fold higher than that of free DOX (Figure S20).

We next investigated whether the current strategy can be utilized for other chemo-drugs with electron donors. First, PBA was allowed to interact with various amines. ^{11}B NMR spectra showed that the chemical shift of PBA in DMF-d_7/D_2O moved to high field after addition of primary, secondary, or tertiary amine, indicating formation of donor−acceptor interaction (Figure 3a). No obvious change of the chemical shift was observed in the case of phenylamine or pyridine, probably due to their weak electron donating ability. Such a result thus indicated the selectivity of donor type toward coordination interaction. Three representative chemo-drugs, epirubicin (EPI), irinotecan (IR), and CPT, were then tested for drug loading in P-PBA micelles. As an analogue of DOX, EPI could be encapsulated with quantitatively high loading (∼51%, Figure 3b). IR, a CPT derivative with tertiary amine, can also be encapsulated with high drug loading. As expected, CPT that lacks electron donors cannot be encapsulated.

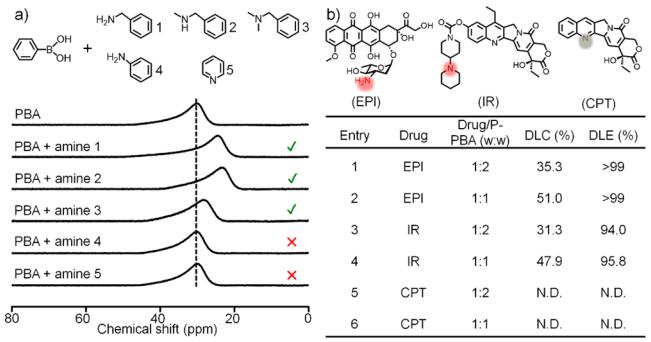

Entry	Drug	Drug/P-PBA (w:w)	DLC (%)	DLE (%)
1	EPI	1:2	35.3	>99
2	EPI	1:1	51.0	>99
3	IR	1:2	31.3	94.0
4	IR	1:1	47.9	95.8
5	CPT	1:2	N.D.	N.D.
6	CPT	1:1	N.D.	N.D.

Figure 3. (a) ^{11}B NMR spectra of the mixture of PBA and different amines (molar ratio = 1:2) in DMF-d_7/D_2O (v/v = 1:2). (b) Drug loading of P-PBA micelles for different chemo-drugs (N.D., not determined due to excessive drug aggregation).

In conclusion, we for the first time reported a convenient strategy to prepare micelles with high drug loading via the incorporation of coordination interactions between electron acceptor-containing polymers and electron donor-containing chemo-drugs. The micelles afforded ultrahigh drug loading (up to 50%) and nearly 100% loading efficiency for various chemo-drugs, along with uniform distribution and desired lyophiliza-

DOI: 10.1021/jacs.7b12776
J. Am. Chem. Soc. 2018, 140, 1235−1238

tion stability. Additionally, the encapsulated drug can be selectively released in response to the high ROS levels in cancer cells. To the best of our knowledge, high drug loading with quantitative loading efficiency has rarely been reported for polymeric micelles with such a convenient method. Without complicated carrier design or drug modification, this approach affords a simple and robust strategy for the encapsulation of hydrophobic drugs, which will benefit further application of polymeric NM.

■ ASSOCIATED CONTENT

Supporting Information

The Supporting Information is available free of charge on the ACS Publications website at DOI: 10.1021/jacs.7b12776.

Experimental procedures and characterizations (PDF)

■ AUTHOR INFORMATION

Corresponding Author

*lcyin@suda.edu.cn.

ORCID

Kaimin Cai: 0000-0001-9442-8312
Xuesi Chen: 0000-0003-3542-9256
Jianjun Cheng: 0000-0003-2561-9291
Lichen Yin: 0000-0002-4573-0555

Notes

The authors declare no competing financial interest.

■ ACKNOWLEDGMENTS

This work was supported by National Natural Science Foundation of China (51403145, 51573123, and 51603137), the Ministry of Science and Technology of China (2016YFA0201200), China Postdoctoral Science Foundation (7131705316), and Priority Academic Program Development of Jiangsu Higher Education Institutions (PAPD).

■ REFERENCES

(1) (a) Kataoka, K.; Harada, A.; Nagasaki, Y. *Adv. Drug Delivery Rev.* **2001**, *47*, 113−131. (b) Peer, D.; Karp, J. M.; Hong, S.; FarokHzad, O. C.; Margalit, R.; Langer, R. *Nat. Nanotechnol.* **2007**, *2*, 751−760. (c) Tong, R.; Hemmati, H. D.; Langer, R.; Kohane, D. S. *J. Am. Chem. Soc.* **2012**, *134*, 8848−8855. (d) Tibbitt, M. W.; Dahlman, J. E.; Langer, R. *J. Am. Chem. Soc.* **2016**, *138*, 704−717. (e) Jeong, K.; Kang, C. S.; Kim, Y.; Lee, Y. D.; Kwon, I. C.; Kim, S. *Cancer Lett.* **2016**, *374*, 31−43.

(2) (a) Sun, R.; Liu, Y.; Li, S.-Y.; Shen, S.; Du, X.-J.; Xu, C.-F.; Cao, Z.-T.; Bao, Y.; Zhu, Y.-H.; Li, Y.-P.; Yang, X.-Z.; Wang, J. *Biomaterials* **2015**, *37*, 405−414. (b) Zhang, F. W.; Zhang, S. Y.; Pollack, S. F.; Li, R. C.; Gonzalez, A. M.; Fan, J. W.; Zou, J.; Leininger, S. E.; Pavia-Sanders, A.; Johnson, R.; Nelson, L. D.; Raymond, J. E.; Elsabahy, M.; Hughes, D. M. P.; Lenox, M. W.; Gustafson, T. P.; Wooley, K. L. *J. Am. Chem. Soc.* **2015**, *137*, 2056−2066.

(3) (a) Tang, L.; Fan, T. M.; Borst, L. B.; Cheng, J. *ACS Nano* **2012**, *6*, 3954−3966. (b) Shi, J.; Kantoff, P. W.; Wooster, R.; Farokhzad, O. C. *Nat. Rev. Cancer* **2017**, *17*, 20−37. (c) Sun, Q. H.; Zhou, Z. X.; Qiu, N. S.; Shen, Y. Q. *Adv. Mater.* **2017**, *29*, 1606628. (d) Hare, J. I.; Lammers, T.; Ashford, M. B.; Puri, S.; Storm, G.; Barry, S. T. *Adv. Drug Delivery Rev.* **2017**, *108*, 25−38. (e) Kamaly, N.; Xiao, Z. Y.; Valencia, P. M.; Radovic-Moreno, A. F.; Farokhzad, O. C. *Chem. Soc. Rev.* **2012**, *41*, 2971−3010.

(4) (a) Prabaharan, M.; Grailer, J. J.; Pilla, S.; Steeber, D. A.; Gong, S. Q. *Biomaterials* **2009**, *30*, 3009−3019. (b) Sun, T. M.; Zhang, Y. S.; Pang, B.; Hyun, D. C.; Yang, M. X.; Xia, Y. N. *Angew. Chem., Int. Ed.* **2014**, *53*, 12320−12364.

(5) (a) Gao, X.; Wang, B. L.; Wei, X. W.; Rao, W.; Ai, F.; Zhao, F.; Men, K.; Yang, B. W.; Liu, X. Y.; Huang, M. J.; Gou, M. L.; Qian, Z. Y.; Huang, N.; Wei, Y. Q. *Int. J. Nanomed.* **2013**, *8*, 971−982. (b) Guha, R.; Chowdhury, S.; Palui, H.; Mishra, A.; Basak, S.; Mandal, T. K.; Hazra, S.; Konar, A. *Nanomedicine* **2013**, *8*, 1415−1428. (c) Wang, H.; Zhao, Y.; Wu, Y.; Hu, Y. L.; Nan, K.; Nie, G.; Chen, H. *Biomaterials* **2011**, *32*, 8281−8290.

(6) (a) Maksimenko, A.; Dosio, F.; Mougin, J.; Ferrero, A.; Wack, S.; Reddy, L. H.; Weyn, A. A.; Lepeltier, E.; Bourgaux, C.; Stella, B.; Cattel, L.; Couvreur, P. *Proc. Natl. Acad. Sci. U. S. A.* **2014**, *111*, E217−E226. (b) Wang, Y. J.; Liu, D.; Zheng, Q. C.; Zhao, Q.; Zhang, H. J.; Ma, Y.; Fallon, J. K.; Fu, Q.; Haynes, M. T.; Lin, G. M.; Zhang, R.; Wang, D.; Yang, X. G.; Zhao, L. X.; He, Z. G.; Liu, F. *Nano Lett.* **2014**, *14*, 5577−5583. (c) Shen, Y. Q.; Jin, E. L.; Zhang, B.; Murphy, C. J.; Sui, M. H.; Zhao, J.; Wang, J. Q.; Tang, J. B.; Fan, M. H.; Van Kirk, E.; Murdoch, W. J. *J. Am. Chem. Soc.* **2010**, *132*, 4259−4265. (d) Cheetham, A. G.; Zhang, P. C.; Lin, Y. A.; Lock, L. L.; Cui, H. G. *J. Am. Chem. Soc.* **2013**, *135*, 2907−2910. (e) Yu, Y.; Chen, C. K.; Law, W. C.; Weinheimer, E.; Sengupta, S.; Prasad, P. N.; Cheng, C. *Biomacromolecules* **2014**, *15*, 524−532.

(7) (a) Yang, C. A.; Tan, J. P. K.; Cheng, W.; Attia, A. B. E.; Ting, C. T. Y.; Nelson, A.; Hedrick, J. L.; Yang, Y. Y. *Nano Today* **2010**, *5*, 515−523. (b) Yang, Y.; Hua, C.; Dong, C. M. *Biomacromolecules* **2009**, *10*, 2310−2318. (c) Li, M.; Tang, Z.; Lv, S.; Song, W.; Hong, H.; Jing, X.; Zhang, Y.; Chen, X. *Biomaterials* **2014**, *35*, 3851−3864.

(8) Cai, K.; He, X.; Song, Z.; Yin, Q.; Zhang, Y.; Uckun, F. M.; Jiang, C.; Cheng, J. *J. Am. Chem. Soc.* **2015**, *137*, 3458−3461.

(9) (a) Mitrasinovic, P. M. *Curr. Org. Synth.* **2012**, *9*, 233−246. (b) Galbraith, E.; James, T. D. *Chem. Soc. Rev.* **2010**, *39*, 3831−3842. (c) Webber, M. J.; Appel, E. A.; Meijer, E. W.; Langer, R. *Nat. Mater.* **2016**, *15*, 13−26. (d) Wani, W. A.; Prashar, S.; Shreaz, S.; Gomez-Ruiz, S. *Coord. Chem. Rev.* **2016**, *312*, 67−98.

(10) Dodge, L.; Chen, Y.; Brook, M. A. *Chem. - Eur. J.* **2014**, *20*, 9349−9356.

(11) Liu, H. L.; Li, Y. Y.; Sun, K.; Fan, J. B.; Zhang, P. C.; Meng, J. X.; Wang, S. T.; Jiang, L. *J. Am. Chem. Soc.* **2013**, *135*, 7603−7609.

(12) (a) Broaders, K. E.; Grandhe, S.; Frechet, J. M. J. *J. Am. Chem. Soc.* **2011**, *133*, 756−758. (b) Wang, M.; Sun, S.; Neufeld, C. I.; Perez-Ramirez, B.; Xu, Q. *Angew. Chem., Int. Ed.* **2014**, *53*, 13444−13448.

(13) (a) Craparo, E. F.; Cavallaro, G.; Bondi, M. L.; Mandracchia, D.; Giammona, G. *Biomacromolecules* **2006**, *7*, 3083−3092. (b) Lv, S. X.; Wu, Y. C.; Dang, J. Q.; Tang, Z. H.; Song, Z. Y.; Ma, S.; Wang, X.; Chen, X. S.; Cheng, J. J.; Yin, L. C. *Polym. Chem.* **2017**, *8*, 1872−1877.

(14) Major Jourden, J. L.; Cohen, S. M. *Angew. Chem., Int. Ed.* **2010**, *49*, 6795−6797.

DOI: 10.1021/jacs.7b12776
J. Am. Chem. Soc. 2018, 140, 1235−1238